An Ultraweak Focusing Storage Ring for Proton EDM Measurement

Richard Talman
Laboratory for Elementary-Particle Physics
Cornell University

4 October, 2017, Juelich

2 Outline

Force Field Symmetries
Why Measure EDM?
Two experiments that "could not be done"
Achievable precision (assuming ***Stern-Gerlach polarimetry*** and ***Phase-locked "Penning-like" trap operation***)
Design requirements for proton EDM storage ring, e.g. at CERN
Proposed ring design ***Weak-weaker WW-AG-CF focusing***
Parameter table
The Brookhaven "AGS-Analogue" electrostatic ring
Off-momentum closed orbits
Potential energy
Ultraweak focusing
Total drift length condition for below-transition operation
Self-magnetometry
Lattice Functions
Heading only—Analytic betatron oscillation description
Heading only—***Virial theorem "absence" of decoherence***
Heading only—***Stochastic cooling stabilization of IBS ?***

3 Force Field Symmetries: Vectors and Pseudovectors

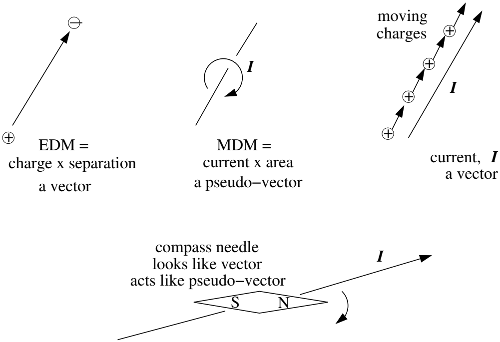

- An electric dipole moment (EDM) points from plus charge toward minus charge—the "orientation" of a true **vector**.
- The axis of a magnetic dipole moment (MDM) is perpendicular to a current loop, whose direction gives a different "orientation". The MDM is a **pseudo-vector**.
- Ampère: how does the compass needle know which way to turn?

4 Capsule history of force field symmetries

- Newton: Gravitational field, (inverse square law) central force
- Coulomb: By analogy, electric force is the same (i.e. central)
- Ampere: How can compass needle near a current figure out which way to turn? Magnetic field is **pseudo-vector**. A **right hand rule** is somehow built into E&M and into the compass needle.
- The upshot: by introducing **pseudo-vector** magnetic field, E&M respects reflection symmetry,
  - but compound objects need not exhibit the symmetry.
  - this was the first step toward the **grand unification** of all forces.
- Lee, Yang, etc: A particle with spin (**pseudo-vector**), say "up", can decay more up than down (**vector**);
  - i.e. the decay vector is parallel (not anti-parallel) to the spin pseudo-vector,
  - viewed in a mirror, this statement is reversed.
  - i.e. weak decay force violates reflection symmetry (P).
- Fitch, Cronin, etc: standard model violates both parity (P) and time reversal (T), so protons, etc. must have both MDM and EDM
- Current task: How to exploit the implied symmetry violation to measure the EDM of proton, electron, etc?

5 Why Measure EDM?

- Violations of parity (P) and time reversal (T) in the standard model are insufficient to account for excess of particles over anti-particles in the present day universe.
- Any non-zero EDM of electron or proton would represent a violation of both P and T, and therefore also CP.

Comments:

- Beam direction reversal is possible in all-electric storage ring, with all parameters except injection direction held fixed. This is crucial for reducing systematic errors.
- "Frozen spin" operation in all-electric storage ring is only possible with electrons or protons—by chance their anomalous magnetic moment values are appropriate. The "magic" kinetic energies are 14.5 MeV for e, 233 MeV for p.

6 EDM Sensitive Configuration—modern day Ampère experiment

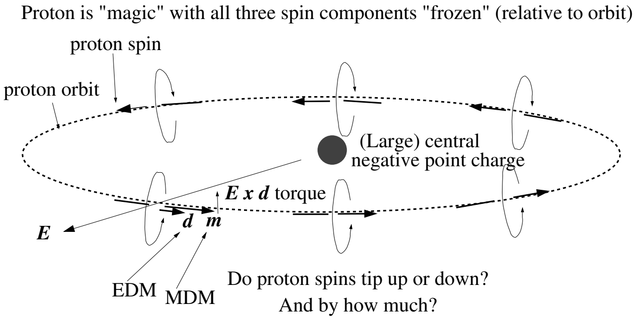

Two issues:

- Can the tipping angle be measurably large for plausibly large EDM, such as 10^{-30} e-cm? With modern, frequency domain, technology, yes
- Can the symmetry be adequately preserved when the idealized configuration above is approximated in the laboratory? *This is the main issue*

7 Two experiments that “could not be done”

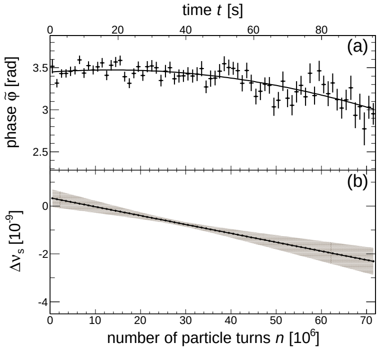

FIG. 3. (a): Phase $\tilde{\varphi}$ as a function of turn number n for all 72 turn intervals of a single measurement cycle for $\nu_s^{\text{fix}} = -0.160975407$, together with a parabolic fit. (b): Deviation $\Delta\nu_s$ of the spin tune from ν_s^{fix} as a function of turn number in the cycle. At $t \approx 38\,\text{s}$, the interpolated spin tune amounts to $\nu_s = (-16097540771.7 \pm 9.7) \times 10^{-11}$. The error band shows the statistical error obtained from the parabolic fit, shown in panel (a).

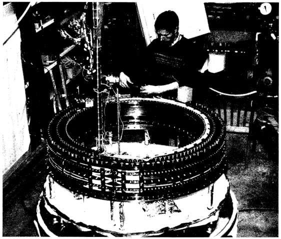

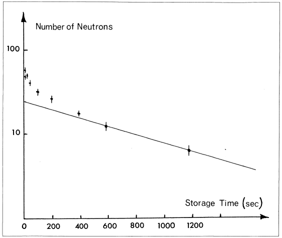

Figure: COSY, Eversmann et al.: (Pseudo-)frozen spin deuterons, and Bonn, Paul et al.: neutron storage ring

8 Achievable precision (assuming perfect phase-lock)

- EDM in units of (nominal value) 10^{-29} e-cm $\equiv \tilde{d}$
- 2 x EDM(nominal)/MDM precession rate ratio:
  $2\eta^{(e)} = 0.92 \times 10^{-15} \approx 10^{-15}$
- duration of each one of a pair of runs $= T_{\rm run}$
- smallest detectable fraction of a cycle $= \eta_{\rm fringe} = 0.001$

$$\begin{aligned} N_{FF} =& \text{EDM induced fractional fringe shift per pair of runs} \\ =& \frac{(2\eta^{(e)})\tilde{d}}{\eta_{\rm fringe}}\, h_r f_0 T_{\rm run} \quad \Big(\overset{\rm e.g.}{\approx}\ \tilde{d}\,\frac{10^{-15}\cdot 10\cdot 10^7\cdot 10^3}{10^{-3}} = 0.1\tilde{d}\Big), \end{aligned}$$

$$\text{Assumed roll rate reversal error } : \pm\eta^{\rm rev.} \overset{\rm e.g.}{=} 10^{-10}$$

$$\begin{aligned} \sigma_{FF}^{\rm rev.} =& \ \ \text{roll reversal error measured in fractional fringes} \\ =& \pm\,\frac{f^{\rm roll}\eta^{\rm rev.}T_{\rm run}}{\eta_{\rm fringe}} \quad \Big(\overset{\rm e.g.}{\approx}\ \pm\frac{10^2\cdot 10^{-10}\cdot 10^3}{10^{-3}} = 10^{-2}\Big). \end{aligned}$$

9 Anticipated precision limit

Space domain, EDM-induced vertical polarization, p-Carbon polarimetry

particle	$\lvert d_{\rm elec}\rvert$ current upper limit e-cm	error after 10^4 pairs of runs e-cm
neutron	3×10^{-26}	
proton	8×10^{-25}	$\pm 10^{-29}$
electron	10^{-28}	$\pm 10^{-29}$

Frequency domain, EDM-induced spin tune shift, phase-locked Stern-Gerlach polarimetry

particle	$\lvert d_{\rm elec}\rvert$ current upper limit e-cm	excess fractional cycles per pair of 1000 s runs	error after 10^4 pairs of runs e-cm	roll reversal error e-cm
neutron	3×10^{-26}			
proton	8×10^{-25}	$\pm 8 \times 10^3$	$\pm 10^{-30}$	$\pm 10^{-30}$
electron	10^{-28}	± 1	$\pm 10^{-30}$	$\pm 10^{-30}$

10 Design requirements for proton EDM storage ring, e.g. at CERN

- Measuring the proton electric dipole moment (EDM) requires an electrostatic storage ring in which 233 MeV, frozen spin polarized protons can be stored for an hour or longer without depolarization.
- The design orbit consists of multiple electrostatic circular arcs
  - Electric breakdown limits bending radius, e.g. $r_0 > 40\,\mathrm{m}$
  - For longest spin coherence time (SCT) and for best systematic error reduction the *focusing needs to be as weak as possible*
  - This is a "worst case" condition for electric and magnetic storage rings to differ (because kinetic energy depends on electric potential energy)
  - To reduce emittance dilution by intrabeam scattering (IBS) the ring needs to operate "below transition"
- Ring must be accurately clockwise/counter-clockwise symmetric
  - Accurately symmetric injection lines are required.
  - Initially single beams would be stored, with run-to-run alternation of circulation directions.
  - Ultimate reduction of systematic error will require simultaneously counter-circulating beams.

11 Proposed ring design ***Weak-weaker WW-AG-CF focusing***

- An ultraweak focusing, "weak/weaker, alternating-gradient, combined-function" (WW-AG-CF) electric storage ring is described.
- All-electric bending fields exist in the tall slender gaps between inner and outer, vertically-plane, horizontally-curved electrodes.

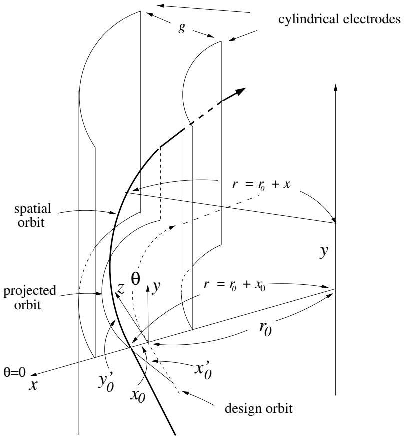

12 Parameter table

Table: Parameters for WW-AG-CF proton EDM lattice

parameter	symbol	unit	value
arcs			2
cells/arc	$N_{\rm cell}$		20
bend radius	r_0	m	40.0
drift length	L_D	m	4.0
circumference	$\mathcal{C}$	m	411.327
field index	m		± 0.002
horizontal beta	β_x	m	40
vertical beta	β_y	m	1620
(outside) dispersion	D_x^O	m	24
horizontal tune	Q_x		1.640
vertical tune	Q_y		0.04045
number of protons	N_p		2×10^{10}
95% horz. emittance	ϵ_x	μm	3
95% vert. emittance	ϵ_y	μm	1
(outside) mom. spread	$\Delta p^O/p_0$		$\pm 2 \times 10^{-4}$
(inside) mom. spread	$\Delta p^I/p_0$		$\pm 2 \times 10^{-7}$

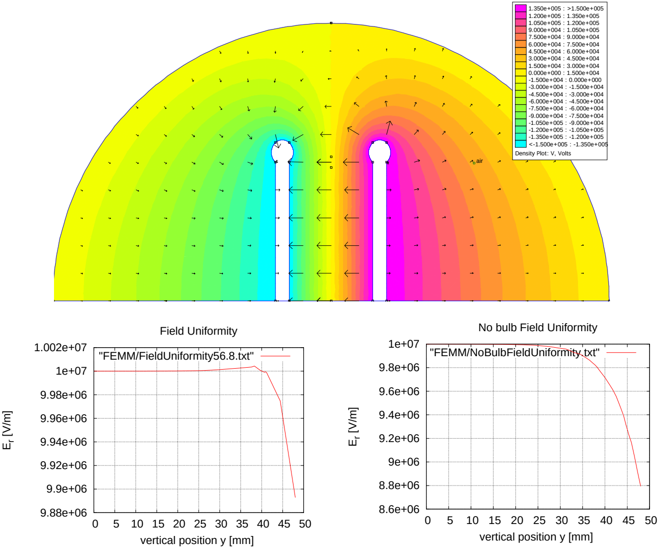

Figure: Above: Electrode edge shaping to maximize uniform field volume; Below left: bulb-corrected field uniformity; Below right: uncorrected field intensity.

- The radial electric field dependence is

$$E = E_r \sim \frac{1}{r^{1+m}},$$

where (ideally) the field index m is exactly $m = 0$.

- $m = 0$ (pure-cylindrical) field produces horizontal bending as well as horizontal "geometric" focusing, but no vertical force
- (Not quite flat) electrode contouring, with m alternating between $m = -0.002$ and $m = +0.002$ provides net vertical focusing.
- Not "strong", this is "weak-weaker" WW-AG-CF focusing, just barely strong enough to keep particles captured vertically.
- Beam distributions are highly asymmetric, much higher than wide, matching the good field storage ring aperture.

- There are no quadrupoles, which is favorable for systematic electric dipole moment (EDM) error reduction.
- *There is no spin decoherence (for frozen spins) in a pure* $m = 0$ *field.*
- The average particle speeds in drift sections do not need to be magic—because there is no spin precession in drift sections.
- Still, the dependence of revolution period on momentum offset is very small, making the synchrotron oscillation frequency small, and not necessarily favorable as regards being above or below transition.
- Below-transition operation requires quite long total drift length

16 The Brookhaven "AGS-Analogue" electrostatic ring

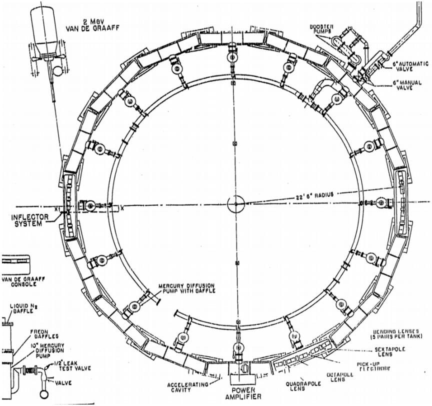

Figure: The 10 MeV "AGS-Analogue" elctrostatic ring has been the only relativistic all-electric ring. It was built in 1954, for U.S.$600,000. It could (almost) have been used to store 15 MeV frozen spin electrons. It was the first alternating gradient ring, the first to produce a "FODO neck-tie diagram", and the first to demonstrate passage through transition (which was its *raison d'être*).

"Magic" central design parameters for frozen spin proton operation:

$$
\begin{aligned}
c &= 2.99792458e8\,\mathrm{m/s} \\
m_p c^2 &= 0.93827231\,\mathrm{GeV} \\
G &= 1.7928474 \\
g = 2G + 2 &= 5.5856948 \\
\gamma_0 &= 1.248107349 \\
\mathcal{E} = \gamma_0 m_p c^2 &= 1.171064565\,\mathrm{GeV} \\
K0 = \mathcal{E} - m_p c^2 &= 0.232792255\,\mathrm{GeV} \\
p0c &= 0.7007405278\,\mathrm{GeV} \\
\beta_0 &= 0.5983790721
\end{aligned}
$$

18 Off-momentum closed orbits

- For central radius r_0 the off-momentum radius is determined by Newton's centripetal force law

$$eE_0 r_0 \left(\frac{r_0}{r}\right)^{1+m} = \frac{\beta_0 p_0 c}{r} \overset{\text{also}}{=} \frac{m_p c^2}{r}\Big(\gamma_0 - \frac{1}{\gamma_0}\Big),$$

  where $r = r_0 + x_D$ is the radius of an off-momentum arc of a circle with the same center.
- For $m \neq 0$, r cancels, and the radius is indeterminant.
- A powerful coordinate transformation is:

$$\xi = \frac{x}{r} = \frac{x}{r_0 + x}$$

- For our typical values ($x = 1\,\text{cm}$, $r_0 = 40\,\text{m}$), for all practical purposes, ξ *can simply be thought of as* x *in units of* r_0..

- The electric field is then

$$\mathbf{E}(\xi) = -E_0\,(1-\xi)^{1+m}\,\hat{\mathbf{r}},$$

- Off-momentum closed orbits are "parallel" arcs of radius $r = r_0 + x_D$ inside a bend, entering and exiting at right angles to straight line orbits displaced also by x_D.
- The relativistic gamma factor on the orbit (inside) is γ^I, which satisfies

$$eE_0 r_0\,(1-\xi)^m = \beta^I p^I c = m_p c^2\Big(\gamma^I - \frac{1}{\gamma^I}\Big),$$

- This is a quadratic equation for γ^I.
- For $r \neq r_0$, because of the change in electric potential at the ends of a bend element, the gamma factor outside has a different value, γ^O.

- For $m \neq 0$ the orbit determination is no longer degenerate.
- Solving the quadratic equation for γ^I, the gamma factor is given by the positive root;

$$\gamma^I(\xi) = \frac{E_0 r_0 (1-\xi)^m}{2m_p c^2/e} + \sqrt{\left(\frac{E_0 r_0 (1-\xi)^m}{2m_p c^2/e}\right)^2 + 1}.$$

- This function is plotted next for $m = \pm 0.2$.

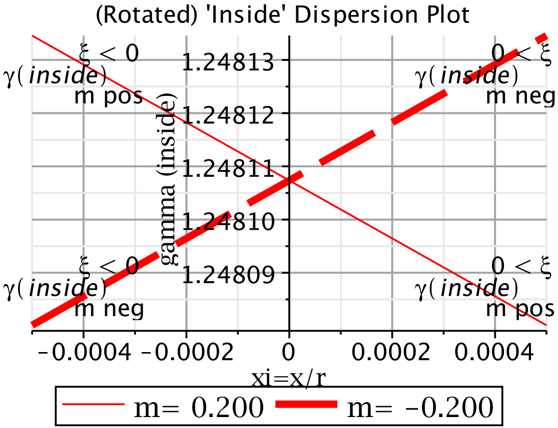

Figure: This figure shows a "dispersion plot" of "inside" gamma value γ^I plotted vs ξ. The curves intersect at the magic value $\gamma^I = 1.248107$. Because $d\gamma/d\beta = \beta\gamma^3$ is equal to about 1.17 at the magic proton momentum, the fractional spreads in velocity, momentum, and gamma are all comparable in value—in this case about $\pm 2 \times 10^{-5}$. This figure may be confusing, since it is rotated by 90 degrees relative to conventional dispersion plots. For this reason one should also study the following plot, which is identical except for being rotated, and is annotated as an aid to comprehension. Subsequent plots have the present orientation, however.

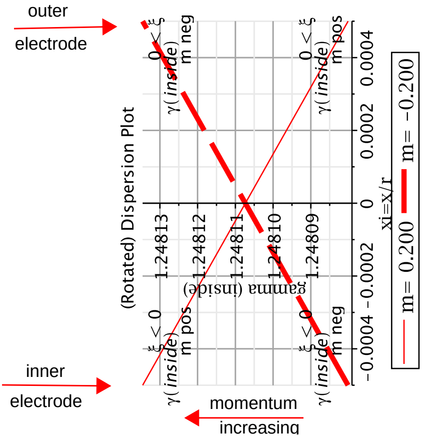

Figure: This plot is identical to the previous one except for being rotated by 90 degrees into conventional orientation (except momentum increases from right to left). It shows the dependence of $\xi = x/r$ vs “inside” gamma value γ^I, for $m = -0.2$ and $m = 0.2$. Note that, for $m < 0$ larger momentum causes larger radius while, for $m > 0$ the opposite is true. *What is striking is that the slope is opposite for $m > 0$ and $m < 0$. This is “anomalous”.*

23 Potential energy

- Electric potential is defined to vanish on the design orbit
- Expressed as power series in ξ, the electric potential is

$$V(r) = -\frac{E_0 r_0}{m}\Big((1-\xi)^m - 1\Big)$$
$$= E_0 r_0\Big(\xi + \frac{1-m}{2}\xi^2 + \frac{(1-m)(2-m)}{6}\xi^3 \dots\Big). \qquad (1)$$

- This simplifies spectacularly for the Kepler m=1 case. But we are concerned with the small $|m| << 1$ case.
- As a proton orbit passes at right angles from outside to inside a bend element, its total energy is conserved;

$$\gamma^O(\xi) = \frac{\mathcal{E}^O}{m_p c^2} = \frac{\mathcal{E}^I}{m_p c^2}$$
$$= \gamma^I(\xi) + \frac{E_0 r_0}{m_p c^2/e}\Big(\xi + \frac{1-m}{2}\xi^2 + \frac{(1-m)(2-m)}{6}\xi^3 \dots\Big).$$

- Plots of $\gamma^O(\xi)$ for $m = \pm 0.2$ are shown next

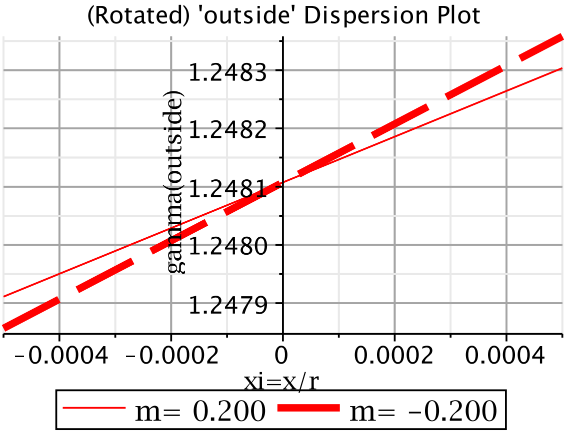

Figure: "Outside" dispersion plots. *Note that dispersion slopes are the same for $m<0$ and $m>0$.* Dependence of "outside" gamma value γ^O on $\xi = x/r$ for $m=-0.2$ and $m=0.2$. Because $d\gamma/d\beta = \beta\gamma^3$ is equal to about 1.17 at the magic proton momentum, the fractional spreads in velocity, momentum, and gamma are all comparable in value—in this case about 2×10^{-4}. *The fractional spreads are an of magnitude greater outside than inside.* This is *helpful*.

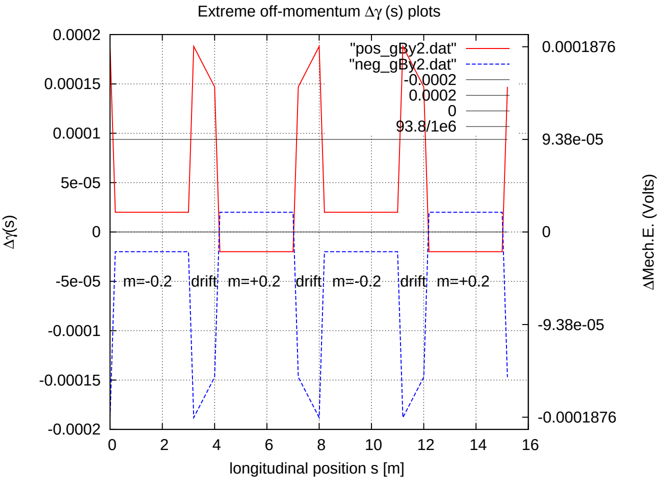

Figure: Dependence of deviation from "magic" $\Delta\gamma(s) = \gamma(s) - \gamma_0$ on longitudinal position s, for off-momentum closed orbits (circular arcs within bends) just touching inner or outer electrodes at $x = \pm 0.015$ m. The right hand tic labels express (approximately) the same quantities as $\Delta\gamma(s) m_p c^2 / e$ mechanical energy offset values. *Notice the anomalous cross-overs in $m > 0$ bends.*

26 Ultraweak focusing

- Figures so far have had $m = \pm 0.2$, which is actually *strong* focusing.
- From now on we assume *ultraweak* focusing with sector values alternating between $m = -0.002$ and $m = 0.002$. The dispersion plots are repeated.

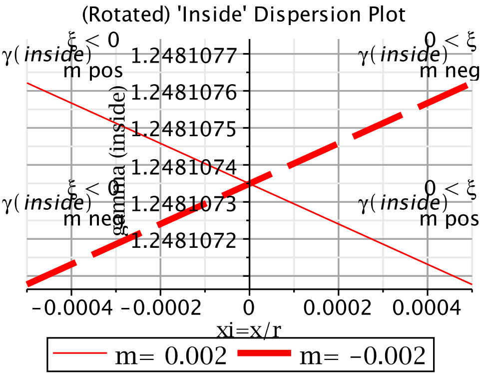

Figure: Dependence of "inside" gamma value γ^I on $\xi = x/r$ for $m = -0.002$ and $m = 0.002$. The curves intersect at the magic value $\gamma^I = 1.248107349$. Because $d\gamma/d\beta = \beta\gamma^3$ is equal to about 1.17 at the magic proton momentum, the fractional spreads in velocity, momentum, and gamma are all comparable in value—in this case about $\pm 3 \times 10^{-7}$—a gloriously small range.

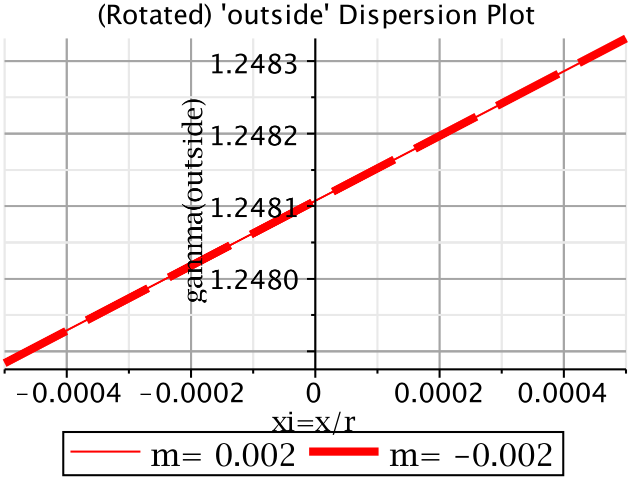

Figure: Dependence of "outside" gamma value γ^O on $\xi = x/r$ for $m = -0.002$ and $m = 0.002$. Because $d\gamma/d\beta = \beta\gamma^3$ is equal to about 1.17 at the magic proton momentum, the fractional spreads in velocity, momentum, and gamma are all comparable in value—in this case about $\pm 2 \times 10^{-4}$. *The fractional spreads are about three orders of magnitude greater outside than inside.*

28 Total drift length condition for below-transition operation

- As with race horses, faster particles can lose ground in the curves but still catch up in the straightaways.
- To run "below transition", the sum of all drift lengths has to exceed $L_D^{\text{trans.}}$, given in terms of dispersion D^O by

$$L_D^{\text{trans.}} = 2\pi D^O \, \beta_0 \gamma_0 \approx 2\pi D^O.$$

Self-magnetometry

- The leading source of systematic error in the EDM measurement is unintentional, unknown, radial magnetic fields.
- Acting on MDM, they cause spurious precession mimicking EDM-induced precession.
- (Apart from eliminating radial magnetic field) the only protection is to measure the differential beam displcement of counter-circulating beams.
- Greatest sensitivity requires weakest verticql focusing.
- i.e. extremely large value for β_y.
- or even octupole-only vertical focusing.

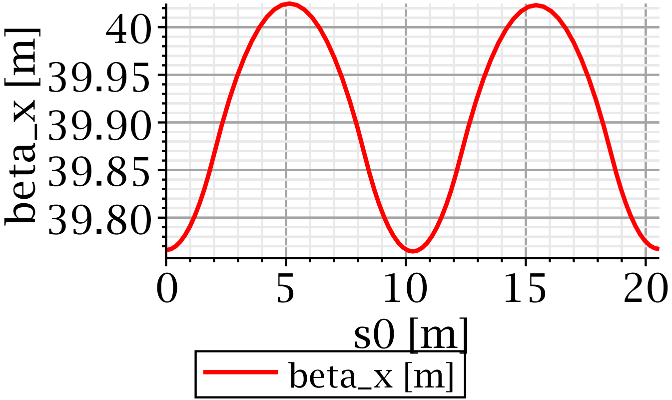

Figure: Horizontal beta function $\beta_x(s)$, plotted for two adjacent cells.

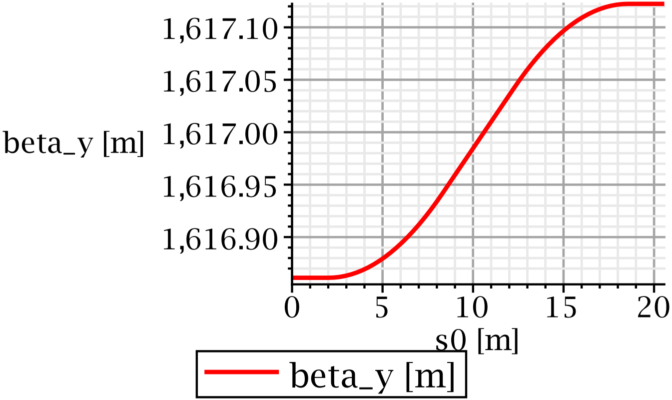

Figure: Vertical beta function $\beta_y(s)$, plotted for two adjacent cells. For this case the total circumference is 411.3 m and the total drift length is 160.0 m. Extended decimal places exhibit the extreme uniformity.

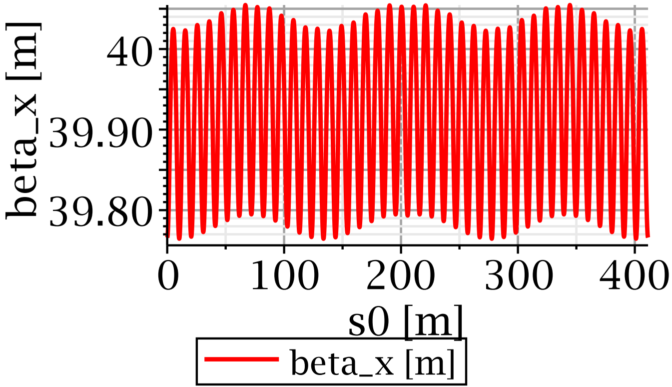

Figure: Horizontal beta function $\beta_x(s)$, plotted for full ring. For this case the total circumference is 411.3 m and the total drift length is L_D=160.0 m. Since this total drift length exceeds $L_D^{\mathrm{trans.}}$, the ring will be "below transition", as regards synchrotron oscillations.

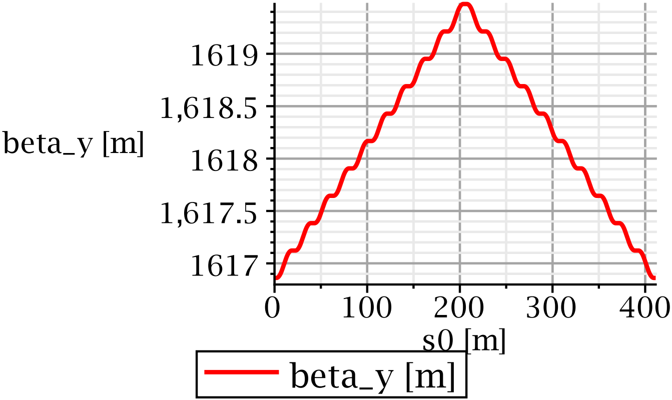

Figure: Vertical beta function $\beta_y(s)$, plotted for full ring. For this case the total circumference is 411.3 m and the total drift length is L_D=160.0 m. Since this total drift length exceeds $L_D^{\mathrm{trans.}}$, the ring will be "below transition", as regards synchrotron oscillations.

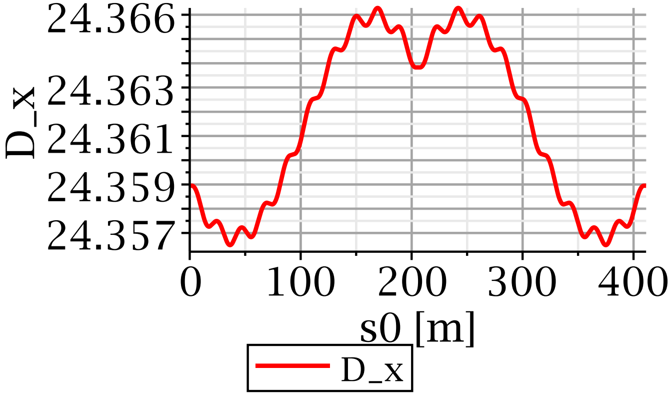

Figure: Outside dispersion function $D^O(s)$, plotted for full ring. For this case the total circumference is 411.3 m and the total drift length is 160.0 m. Extended decimal places exhibit the extreme uniformity.

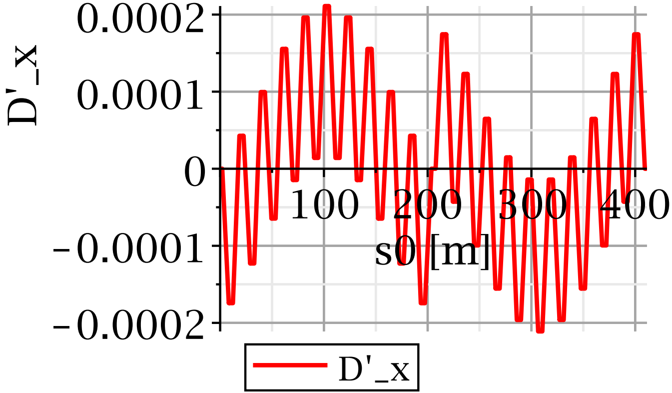

Figure: Outside dispersion function slope $D^O(s)'$, plotted for full ring. For this case the total circumference is 411.3 m and the total drift length is 160.0 m.

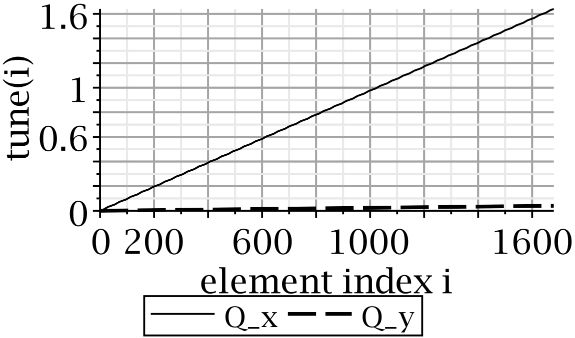

Figure: Transverse tune advances. The full lattice tunes are $Q_x = 1.640$ and $Q_y = 0.04046$. Even smaller horizontal tune (for improved self-magnetometry) can be provided by trim quadrupoles. If possible, rather than by vertical electrode-contouring, the vertical field contouring will be provided electrically, and be consistent with zero quadrupole focusing, but withoctupole focusing for net vertical stability.

- R. Talman, *The Electric Dipole Moment Challege,* IOP Publishing, 2017
- R. and J. Talman, *Symplectic orbit and spin tracking code for all-electric storage rings,* Phys. Rev. ST Accel Beams **18**, ZD10091, 2015
- R. and J. Talman, *Electric Dipole Mومment Planning with a resurrected BNL Alternating Gradient Synchrotron electron analog ring,* Phys. Rev. ST Accel Beams **18**, ZD10092, 2015
- R. Talman and J. Talman, *Octupole focusing relativistic self-magnetometer electric storage ring bottle,* arXiv:1512.00884-[physics.acc-ph], 2015
- C. Møller, *The Theory of Relativity,* Clarendon Press, Oxford, 1952